

## 7.1

### Quantum Standards for Voltage

Johannes Kohlmann

#### 7.1.1

##### Introduction

About 50 years ago, in 1962, Brian Josephson [1] set the cornerstone for a revolution in the field of electrical high-precision measurements by his seminal paper on superconductive tunneling. Since then, Josephson junctions (JJs) consisting of two weakly coupled superconductors became the basis for most applications of superconductive electronics (cf. [2]). In electrical metrology, being the science of high-precision measurements, voltage standards based on JJs are nowadays used as quantum standards for the electrical voltage in many laboratories worldwide for high-precision measurements.

While these standards are conceptually simple, about 50 years of developments were needed to progress from Josephson's idea to modern Josephson voltage standards (JVSs). This long period has been caused by the need for both new ideas and a significant progress of the fabrication technology. The advanced thin-film technology is a major precondition for modern JVSs, as their main component is a highly integrated series array of JJs. Its improvements made the progress from single JJs delivering a few millivolts to large series arrays for output voltages above 10 V containing 100 000 JJs or more possible. While JVSs were initially used for DC applications, their enormous capabilities for AC voltage metrology were demonstrated in recent investigations with new measurement tools developed since the mid-1990s.

This chapter describes the development and present status of JVSs focused on modern AC JVSs. Numerous review papers have been published in the course of time covering different topics of JVSs, for example, DC JVSs [3–6], the physics underpinning DC JVSs [7], the transition from DC to AC JVSs [8–14], the physics underpinning AC JVSs [15], and an overview focused on the historical developments [16].

#### 7.1.2

##### Fundamentals

After a brief discussion of physical units in general and the electrical unit volt in particular, some fundamentals and the developments from the Josephson effect to modern JVSs are summarized in this section. Detailed descriptions of the Josephson effects and JJs are given in other chapters of this book and have been reviewed in several papers [4, 17, 18] and textbooks [19–21].

##### 7.1.2.1 Measurements, Units, and the SI

Each kind of measuring requires a reproducible system of measurement including suitable units. The modern system of measurement is the International System

of Units, universally abbreviated SI (from the French Le Système International d'Unités) [22]. Of the seven base units in the SI, only the ampere relates to electrical measurements. The unit of voltage, the volt, belongs to the derived units.

The definition of the volt is based on the coherency of electrical power  $P_{el} = I \cdot V$  (current times voltage) and mechanical power  $P_m = F \cdot l/t$  (force times distance divided by time). *One volt* is defined as the difference in electric potential along a wire when an electric current of 1 A dissipates 1 W of power (cf. [en.wikipedia.org/wiki/Volt](http://en.wikipedia.org/wiki/Volt)):  $1 \text{ V} = 1 \text{ N m (A s)}^{-1}$ . Therefore, the realization of the volt in the SI depends on experiments that relate electrical units to mechanical units, which is made, for example, using an extremely difficult to handle voltage balance [23]. While the definition of the volt in the current SI is completely independent from the Josephson effect, this might change in future with a new definition of some SI units [24].

A complex measurement equipment as the voltage balance is not suitable for routine use as calibrations. For this purpose, voltage standards are required enabling the generation of stable and reproducible voltages. These standards are said to represent the volt. For several decades until 1972, this representation of the volt was made by Weston cells, a wet-chemical Cd–Hg cell delivering about 1.018 V [25]. With increasing requirements for precision measurements, the representation of the volt by an artifact showed its drawbacks like damage by improper handling and dependence of measurements on external parameters among others. In addition, international intercomparisons were difficult because of transport problems. In contrast, a quantum standard as the JVS relates the unit volt to fundamental constants and a frequency and subsequently allows the determination of voltages independently of time and space.

These advantages of quantum standards have been used since 1972, when a value for the Josephson constant  $K_J = 2e/h$  was recommended for use in realizing and maintaining accurate and stable representations of the volt for the first time ( $e$  is the elementary charge and  $h$  Planck's constant). While most National Metrology Institutes (NMIs) adopted the value of  $483\,594.0 \text{ GHz V}^{-1}$ , three did not and used a slightly different value (the United States, France, and USSR) [26, 27]. This disappointing situation causing different representations of the volt was not solved until 1990, when a new value of the Josephson constant was adopted by all NMIs:  $K_{J,90} = 483\,597.9 \text{ GHz V}^{-1}$  [28].

### 7.1.2.2 Josephson Effects and Voltage Standards

Josephson theoretically investigated the behavior of two weakly coupled superconductors [1] on the basis of the BCS theory by Bardeen, Cooper, and Schrieffer [29]. He predicted two effects related to the tunneling of Cooper pairs across the weak link in dependence of the phase difference  $\phi$  between the macroscopic wave functions of the two superconductors: the DC Josephson effect depicts a DC supercurrent  $I = I_c \cdot \sin \phi$  that can flow across the junction at zero voltage ( $I_c$  denotes the critical current). The AC Josephson effect describes an AC supercurrent of frequency  $f_j = (2e/h)V$ , if the junction is operated at a finite voltage  $V$ . As already discussed by Josephson in his first paper [1], external microwaves

of frequency  $f$  can phase-lock the Josephson oscillator over a certain bias current range and thus generate constant-voltage steps  $V_n$ :  $V_n = n \cdot (h/2e)f$  ( $n = 1, 2, 3, \dots$ ). The generation of these steps can alternatively be illustrated as a transfer of magnetic flux quanta  $\Phi_0 = h/2e$  across the JJ.

The reproduction of voltages is thus reduced to the determination of a frequency, which can be precisely controlled by and accurately referenced to atomic clocks. The first experimental confirmation of constant-voltage steps was performed by Shapiro in 1963 [30]; these steps are therefore often entitled as *Shapiro steps*. A single JJ irradiated by 70 GHz microwaves generates a voltage of only  $145 \mu\text{V}$ , when operated on the first-order step ( $n = 1$ ). This voltage level is too low for most applications, even for higher order steps. Reference voltages of 1 V or even 10 V as needed for real applications cannot be generated by a single junction but only by large series arrays of  $M$  JJs:

$$V_n = n \cdot M \cdot \Phi_0 \cdot f \quad (7.1.1)$$

Equation (7.1.1) relating voltages to frequencies is the physical basis of JVs. DC voltages of conventional JVs are generated with  $n$ ,  $M$ , and  $f$  fixed. The voltages become time dependent, when the number of junctions  $M$  or the frequency  $f$  is varied over time. Both alternatives have been realized and investigated: the number of junctions  $M$  is altered in binary-divided arrays and the frequency  $f$  in pulse-driven arrays.

The dynamics of a JJ is often described using the resistively capacitively shunted junction (RCSJ) model first proposed by Stewart and McCumber in 1968 [31, 32]. The real JJ is here represented by an ideal Josephson element shunted by an ohmic resistance  $R$  and a capacitance  $C$ . In the linear approximation, the resonance frequency of this parallel circuit is given by the plasma frequency  $f_p = (e \cdot j_c / \pi \cdot h \cdot C_s)^{1/2}$  of the JJ ( $j_c$  denote the critical current density,  $C_s = C/A$  the specific junction capacitance, and  $A$  the junction area). Details of the electrical behavior depend on the kind of the junction, which can be characterized by the dimensionless McCumber parameter  $\beta_c = Q^2$  being equal to the square of the quality factor  $Q = 2\pi \cdot f_p \cdot R \cdot C$  of the junction. Two kinds of junctions are distinguished, namely underdamped junctions with  $\beta_c > 1$  and overdamped junctions with  $\beta_c \leq 1$ , respectively. The current–voltage ( $I$ – $V$ ) characteristics of these junctions significantly differ as schematically illustrated in Figure 7.1.1: underdamped junctions show a hysteretic  $I$ – $V$  characteristic and overdamped junctions a nonhysteretic one. These differences in the  $I$ – $V$  characteristic remain also visible under microwave irradiation (cf. Figure 7.1.1), while underdamped junctions show overlapping Shapiro steps when irradiated at low microwave power, the steps of overdamped junctions as well as of underdamped junctions if irradiated with high microwave power are single valued. The step width depends on the microwave power received by the junctions; in some cases, this dependence is given by a Bessel function [4, 7].

The characteristics of the JJs also determine their behavior under microwave irradiation (cf. [4, 7, 15]). An important parameter here is the characteristic voltage  $V_c = I_c \cdot R_n$  ( $R_n$  denotes the normal state resistance of the JJs). The

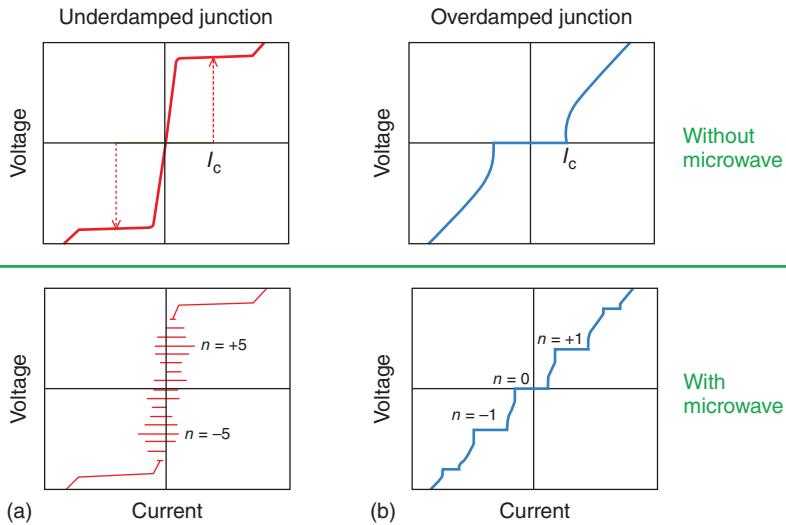


**Figure 7.1.1** Schematic  $I$ - $V$  characteristics of underdamped (a) and overdamped (b) JJs without (top) and with (bottom) microwave irradiation. Some constant-voltage steps are marked. The microwave power is set to optimized operation.

characteristic voltage is related to the characteristic frequency  $f_c$  by Eq. (7.1.1):  $f_c = (2e/h) \cdot V_c = (2e/h) \cdot I_c \cdot R_n$ . The frequency of the external drive should be near the characteristic frequency in particular for JVSs based on overdamped JJs [15].

### 7.1.2.3 From Josephson Effects to Modern JVSs

The current status of JVSs is the result of research and developments over more than 50 years. This period of time can be subdivided into five stages each lasting about a decade. The transition to the next stage has often been related to new ideas or new technological achievements.

The first decade was determined by investigations of single JJs confirming the Josephson effects and performing first precision experiments. At that time, the deployed junctions (weak links) consisted of point contacts, microbridges, SNS, or SIS junctions (S, superconductor; I, insulator; N, normal metal). While the Josephson effect was initially used to improve the measurement of the fundamental constant  $2e/h$ , the application for voltage standards came more and more to the fore as first suggested by Taylor *et al.* in 1967 [33]. In addition, the universality of the Josephson effect was proven with increasing accuracy from Clarke in 1968 to Jain *et al.* in 1987 [34, 35] to parts in  $10^{19}$ .

In the second decade until the early 1980s, single SIS junctions were really used as voltage standards. A few millivolts were delivered by the underdamped junctions operated on higher order constant-voltage steps under irradiation of high microwave power at a frequency around 10 GHz. This period was terminated by the challenging trial to increase the output voltage; a series array of 20 individually biased JJs delivered an output voltage of about 100 mV by Endo *et al.* in 1983 [36].

While the idea of series arrays of thousands of JJs was rather bizarre in the 1970s, the situation changed at the beginning of the third decade in the early 1980s (for reviews, cf. [3, 4, 37]), when the chapter of modern JVSs was opened by two new ideas. First, Levinsen *et al.* [38] suggested in 1977 the use of zero-current constant-voltage steps of highly underdamped junctions operated at low microwave power instead of the use of normal steps observed at high microwave power used so far. For the first time, series arrays of JJs could be operated by a single-bias source only, because the current ranges of the constant-voltage steps do overlap one another for small bias currents. Second, the Physikalisch-Technische Bundesanstalt (PTB) in Germany suggested to embed large series arrays of JJs into an adapted microwave transmission line (microstrip line). First 1 V arrays of more than 1000 junctions were realized within a cooperation between the National Bureau of Standards (NBS; now National Institute of Standards and Technology, NIST) in the United States and the PTB by Niemeyer *et al.* in 1984 [39]. The integrated microwave circuit allows a series connection of the JJs for the DC bias and a parallel connection of several microstrip line paths with respect to the microwave drive and is still used to date for 70 GHz circuits in both conventional and programmable Josephson voltage standards (PJVSs). First 10 V arrays containing a further increased number of junctions were realized a few years later [40, 41]. These conventional JVSs for operation at 70 GHz became more and more widespread and are nowadays operated in more than 50 labs worldwide for DC measurements (cf. Section 7.1.3). The progress of JVSs is intimately linked with significant improvements of the thin-film technology, to enable the fabrication of highly integrated circuits containing thousands of JJs similar to procedures of semiconductor industry.

In the fourth decade in the 1990s, the development of conventional JVSs was largely completed by launching commercially available systems. While several companies have sold these systems over the years, two companies<sup>1)</sup> offer them at present. In parallel, the fundamentals for the next generation of JVSs were developed and investigated, namely AC JVSs. For this purpose, a new junction type and novel operation principles were required, as conventional JVSs do not enable rapid and reliable switching between different specific voltage levels due to their complex overlap. Moreover, the chaotic behavior of underdamped junctions leads to a certain instability of the constant-voltage steps (cf. [4, 7]). The increasing interest in rapidly switching arrays and in highly precise AC voltages resulted in two different main developments: the PJVS suggested by Hamilton *et al.* in 1995 [42] and the pulse-driven Josephson arbitrary waveform synthesizer (JAWS) suggested by Benz and Hamilton in 1996 [43] (cf. Section 7.1.4).

While in the fourth decade, the development and first experiments at 1 V using PJVS and at low voltage levels using JAWS were in the focus of research, in the fifth and for now last decade starting in the early 2000s, the application of JVSs has been really extended from DC to AC more and more also at 10 V (PJVS). The activities were focused on JJs showing nonhysteretic  $I$ - $V$  characteristics typical

1) Hypres Inc., USA: [www.hypres.com](http://www.hypres.com) and Supracon AG, Germany: [www.supracon.com](http://www.supracon.com).

for overdamped junctions realized, for example, by SNS or SINIS junctions. Their Shapiro steps are single valued, that is, the steps do not overlap, and are consequently inherently stable. As the junctions are typically operated on the first-order step, the number of junctions needed for 1 V or even 10 V arrays have significantly increased compared to conventional SIS arrays. Depending on the drive frequency, the circuits consist of about 70 000 junctions (10 V, 70 GHz) and 300 000 junctions (10 V, 15 GHz), respectively. A significantly improved fabrication technology as well as sophisticated microwave designs has been required for the successful development of these giant series arrays. Numerous examples demonstrate the promising capabilities of Josephson arrays for AC applications. However, already the first experiments showed that high-precision AC experiments require much more effort than DC experiments (cf. Section 7.1.4).

### 7.1.3

#### DC Measurements: Conventional Josephson Voltage Standards

As already mentioned in Section 7.1.2, the development of modern JVSs for output voltages of 1 V or even 10 V was enabled by two new ideas around 1980, namely the use of highly underdamped JJs and their integration into a low-impedance microstrip line [39]. While more than 1000 JJs are already required for 1 V arrays, 10 V arrays typically contain between 14 000 and 20 000 JJs [44–48]. The uniform microwave power distribution over all JJs is an essential requirement for the designs of series arrays to enable the generation of wide and stable constant-voltage steps. The underdamped JJs are realized by SIS junctions for operation at microwave frequencies around 70 GHz. On average, each junction of the array is operated on the fifth constant-voltage step, which kept the required junction number to an acceptable value for the fabrication technology available at that time.

For SIS junctions, the ohmic resistance  $R_n$  is about  $50 \Omega$ , while the impedance of the capacitive branch  $Z_d = 1/(2\pi \cdot f \cdot C)$  is about  $50 \text{ m}\Omega$  for a junction capacitance of  $50 \text{ pF}$ . High-frequency currents, therefore, flow mainly capacitively resulting in a very low attenuation of the microwave power from about 1 dB per 1000 junctions to 2 dB per 1000 junctions. Each branch of the microstrip line can, therefore, contain a lot of junctions (about 3500 junctions in the real PTB design) without losing a uniform microwave power distribution to each junction. Another microwave line was recently suggested by Schubert *et al.* [49], who integrated the SIS junctions into a coplanar stripline (CPS) with an impedance of  $50 \Omega$ . More details of microwave circuits are discussed in Section 7.1.4.1.1.

In the 1980s, JJs and first series arrays were fabricated in lead/lead alloy technology (cf. [39]); but the crucial problem was the susceptibility to damage of the lead alloy circuits by humidity and thermal cycling. Another technology at that time was based on JJs made of Nb/Nb<sub>2</sub>O<sub>5</sub>/PbBi [40]. The main breakthrough in the development of a robust fabrication process was the invention of the Nb/Al–Al<sub>2</sub>O<sub>3</sub> technology by Gurvitch *et al.* in 1983 [50]. This technology

combines the use of the durable and chemically stable metal Nb with the high critical temperature of about 9.2 K, the outstanding covering of thin Al layers on Nb, and the formation of a very homogeneous and stable oxide of Al by thermal oxidation. The thickness of the oxide barrier is about 1 nm, and that one of the superconductive layers more than 150 nm and therefore roughly twice the superconducting penetration depth at least. For a reliable process, the trilayer defining the junctions is deposited as a sandwich structure without breaking the vacuum. The adaptation of this process made possible the fabrication of JVS arrays consisting of Nb/Al–Al<sub>2</sub>O<sub>3</sub>/Nb JJs in 1986 [51]. Nowadays, all series arrays for JVSs are fabricated in processes fundamentally based on this invention.

Dielectric layers are made of SiO<sub>2</sub>. Optical or electron-beam lithography is used. The different layers are patterned by adapted fluorine-based dry etching processes. The size of the JJs is limited to about 20 μm in length and 50 μm in width because of some restrictions to assure stable operation [4]. A critical current density of <math><40 \text{ A cm}^{-2}</math> results in critical currents of a few hundreds of microamperes at most and up to 50 μA width of the constant-voltage steps (cf. [5]). More than 50 conventional JVSs are presently in operation at NMIs, calibration laboratories [52], and instrumentation manufactures (cf. [53]). Typical 10 V systems provide a combined uncertainty of between a few parts in 10<sup>10</sup> and a few parts in 10<sup>11</sup> (cf. [52, 54]). Their widespread use was significantly supported by the commercial availability of turn-key systems as that shown in Figure 7.1.2 as an example.



**Figure 7.1.2** Photograph of a commercial cryocooler-based Josephson voltage standard system. (Courtesy of Supracon AG.)

## 7.1.4

## From DC to AC Josephson Voltage Standards

In the mid-1990s, the increasing interest in rapidly switching arrays and in highly precise AC voltages stimulated the development of series arrays based on JJs showing a nonhysteretic  $I-V$  characteristic, as conventional JVSs do not allow rapid switching between different constant-voltage steps. The  $I-V$  characteristic of these overdamped JJs remains single valued under microwave irradiation (cf. Figure 7.1.1). Consequently, the constant-voltage steps are inherently stable and can be rapidly selected by external biasing.

Different versions of AC quantum voltage standards were suggested and partly realized since the mid-1990s. The most important ones are JVSs based on binary-divided arrays (cf. Section 7.1.4.1) and pulse-driven arrays (cf. Section 7.1.4.2). Moreover, digital-to-analog converters based on the dynamic logic of processing single-flux quanta (SFQ) were investigated (cf. [55]). This SFQ version was realized only for small output voltages because of the enormous complexity of the required circuits. In the following, the first two versions are described in more detail, as most research activities are presently focused on these two.

## 7.1.4.1 Binary-Divided Arrays

PJVSs are based on binary-divided series arrays of JJs and are operated as multibit D/A converters with fundamental accuracy [42]. The series array of  $M$  total junctions is divided into smaller independently biased segments (cf. Figure 7.1.3). The number of junctions per segment often follows a binary sequence. The output voltage  $V_n = n \cdot M \cdot \Phi_0 \cdot f$  is given by digitally programming the step number  $n$  for the junctions in each segment (typically  $n = -1, 0, +1$ ). Each constant-voltage step between  $-M$  and  $+M$  can be selected by suitable programming of the different segments using a fast bias electronics. Binary-divided arrays have further enlarged the requirements for the fabrication technology because of the increased number of JJs, as PJVSs are typically operated on the first-order constant-voltage step instead of the fifth one for SIS arrays, and because the constant-voltage steps appear at finite bias currents so that parameter deviations of the JJs result in reduced step widths for series arrays.

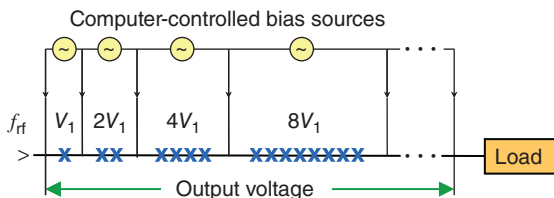


**Figure 7.1.3** Schematic of a programmable JVSs based on a binary-divided series array of Josephson junctions shown as X. The array is operated as a multibit D/A converter.



#### 7.1.4.1.1 Design of Binary-Divided Arrays

The microwave circuit designs of modern JVSs are based on one of three different microwave lines: low-impedance microstrip line,  $50\ \Omega$  coplanar waveguide transmission line (CPW), and  $50\ \Omega$  CPS. PJVSs operated in the frequency range from 10 to 20 GHz are mainly based on CPWs (cf. [56–58]). CPW and CPS offer the advantage of a simpler fabrication technology compared to the microstrip line that needs an additional ground plane and a dielectric layer. Besides excellent transmission characteristics around 70 GHz, the microstrip line makes a rather simple splitting of a single high-frequency line in two parallel ones possible; by making use of DC blocks, this splitting can be performed several times. Therefore, the junctions are distributed over a certain number of short parallel microwave paths instead of over one very long path. Each microwave branch is terminated by a matched lossy microwave line that serves as a load, which provides a uniform microwave distribution by suppressing microwave reflections with standing waves.

As an example, the PTB design of a 10 V SNS array for operation at 70 GHz is shown in Figure 7.1.4. An antipodal finline taper serves as an antenna. It connects the microstrip line with the JJs to the E-band rectangular waveguide of the cryoprobe by matching the impedance of the waveguide (about  $520\ \Omega$ ) to that of the microstrip line (about  $5\ \Omega$ ). Details of the design are determined by the high-frequency behavior of the JJs.

In comparison with underdamped JJs of conventional JVSs, the microwave conditions are completely different for overdamped junctions embedded into a microstrip line. Now,  $R_n$  and  $Z_d$  are comparable (about  $50\ \text{m}\Omega$  each) leading to the significant dissipation of the microwave current and thus to a significant attenuation of the microwave power of about 50 dB per 1000 junctions (cf. [59]). The high attenuation, however, is partly compensated by an active contribution

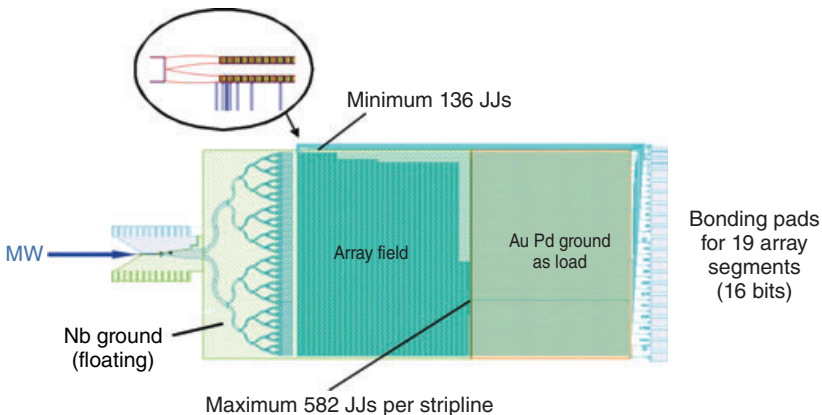


**Figure 7.1.4** Design of a 10 V SNS Josephson series array developed at PTB. The array consists of 69 632 junctions embedded into 128 parallel low-impedance microstrip lines.

The length and width of a single junction is  $6\ \mu\text{m} \times 20\ \mu\text{m}$ . The size of the total chip is  $24\ \text{mm} \times 10\ \text{mm}$ .

of the junctions; the junctions act as oscillators. The single microwave paths of programmable series arrays consist of 128 junctions (1 V design) and up to 582 junctions (10 V design). Therefore, the microwave circuit of a 1 V array consists of 64 parallel paths, and that of a 10 V array consists of 128 paths.

A contrary situation is found for overdamped SNS junctions embedded into the middle of a CPW as realized at NIST. The large ratio of the low junction impedance to the  $50\ \Omega$  impedance of the CPW leads to a situation that is similar to that of the microstrip line for conventional SIS arrays: the attenuation of the microwave power is low, because the junctions are loosely linked to the CPW. The integration of much more junctions in a single microwave path is therefore possible than in the case of microstrip line designs. Typical numbers for 1 V (10 V) arrays are 8 (32) branches containing 4096 (8400) junctions each [57, 60].

As chaos is suppressed in overdamped junctions, the limitations for their sizes are less strict. Typical sizes of the JJs are between a few micrometers and some tens of micrometers. Critical current densities between some kiloampere per square centimeter and some  $10\ \text{kA cm}^{-2}$  result in critical currents up to about 10 mA and step widths of several milliamperes (cf. [15]).

#### 7.1.4.1.2 Realization of Binary-Divided Arrays

The PJVS was suggested and first demonstrated by Hamilton *et al.* at NIST in 1995 [42]. In this proof-of-concept experiment, 2048 junctions of an array containing 8192 externally shunted SIS junctions were operated at 75 GHz and delivered a maximum DC voltage of about 300 mV. They also presented first AC voltages in the kilohertz range at  $\pm 77\ \text{mV}$  with  $150\ \mu\text{V}$  resolution. As design restrictions of externally shunted SIS junctions limited the critical current and consequently the step width to a few hundred microamperes, other junction types have subsequently been investigated. The final breakthrough of programmable voltage standards was enabled by the implementation of SNS junctions by Benz [56] based on calculations by Kautz [15].

The first practical 1 V arrays were realized by Benz *et al.* in 1997 [57]. A total of 32 768 SNS junctions containing PdAu as the normal metal were embedded into the middle of a CPW with an impedance of  $50\ \Omega$ . Under microwave operation around 16 GHz, the width of the constant-voltage steps exceeds 1 mA. The low microwave frequency is determined by the low characteristic voltage of typical SNS junctions because of the low resistivity of the normal metal.

Different materials for the normal metal were investigated as Ti [61],  $\text{MoSi}_2$  [62], or TiN [63]. In search of other materials showing a high resistivity, a new type of junction has increasingly gained importance recently: its barrier consists of a semiconductor such as Si doped with a metal and being near a metal–insulator transition [64]. Although these junctions mainly behave like SNS junctions, their characteristics are more determined by the semiconductor and the interfaces to the superconductors. A promising version of these junctions was first realized by an amorphous Si barrier doped by Nb at NIST in 2006 [64]. Nb and Si are cosputtered from two sputter targets; the Nb content is varied by adjusting the power for sputtering. If the niobium content is tuned to a value near the metal–insulator

transition around 11.5% [65],  $\text{Nb}_x\text{Si}_{1-x}$  barriers with a thickness between 10 and 30 nm combine a high resistivity and a sufficient conductivity.

The low drive frequency around 16 GHz requires 32 000 JJs to reach 1 V and even about 300 000 JJs for 10 V. These huge numbers of junctions cause enormous challenges for the microwave design and the fabrication technology. To reduce the size of these circuits, the use of double- and triple-stacked junctions was subsequently investigated [62, 63, 66]. Burroughs *et al.* [66] demonstrated 10 V arrays containing three-junction stacks with 268 800  $\text{Nb}_x\text{Si}_{1-x}$  barrier junctions arranged in 32 parallel branches in 2009. To assure a homogeneous microwave power distribution along 8400 junctions in each branch, the microwave design was further improved including tapered CPWs and modified power dividers at the splitter stages [58, 67]. Step widths above 1 mA at 10 V were generated under microwave irradiation near 20 GHz [66, 68]. Recently, Fox *et al.* [69] analyzed the junction yield of these series arrays: the average number of defects per million junctions was 32.5 considering series arrays from nine wafers with a total of 25 346 652 junctions corresponding to a total average junction yield of 99.9967%.

The PTB group took a different path. In order to decrease the number of junctions necessary to reach a given voltage, the operation frequency must be increased, which requires junctions with a larger characteristic voltage. A promising approach for operation at 70 GHz like the conventional JVs was the development of SINIS junctions ( $\text{Nb}/\text{Al}_2\text{O}_3/\text{Al}/\text{Al}_2\text{O}_3/\text{Nb}$ ) originally investigated for electronic applications in Japan in 1997 [70, 71]. The fabrication is comparable to that of conventional SIS arrays. Small series arrays and 1 V arrays containing 8192 junctions were subsequently fabricated at PTB by Schulze *et al.* [72] and Behr *et al.* [73]. The first 10 V arrays consisting of 69 120 junctions were developed shortly after by Schulze *et al.* in 2000 [74] and later significantly improved for AC applications by Müller *et al.* [75].

However, a serious drawback of SINIS junctions is their sensitivity to particular fabrication processes often resulting in a few shorted junctions of a SINIS series array (typically between 0 and 2 of 10 000 junctions) probably caused by the very thin insulating oxide barriers (cf. [76]). While pure metallic SNS junctions are not really suitable for operation at 70 GHz,  $\text{Nb}_x\text{Si}_{1-x}$  barrier junctions allowed the fabrication of 1 and 10 V arrays for operation at 70 GHz, as first demonstrated by Mueller *et al.* in 2008 [76] within a cooperation between NIST and PTB. Some 10 V arrays consisting of 69 632 junctions were realized without any shorted junction, an array quality that had never been achieved using SINIS junctions. Step widths above 1 mA for 10 V arrays have meanwhile been reached as shown in Figure 7.1.5. Using double-stacked junctions, first arrays delivering output voltages of 20 V have also been realized [77].

While  $\text{Nb}_x\text{Si}_{1-x}$  barrier junctions currently enable the most reliable fabrication process for 1 and 10 V arrays, some other kinds of junctions have also been investigated in recent years. With the aim of constructing compact and low-cost PJVs, Yamamori *et al.* [78] developed arrays that can be operated in a compact cryocooler at temperatures around 10 K using NbN for the superconducting layers and TiN for the barrier. The arrays consisting of more than 500 000 junctions

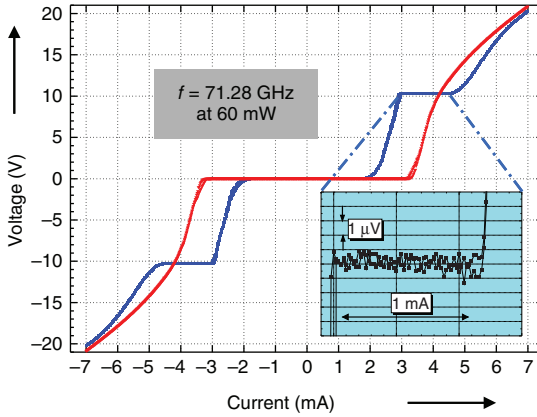


**Figure 7.1.5**  $I$ - $V$  characteristic of a 10 V PJVS of PTB without (red) and with (blue) 70 GHz microwave irradiation. The inset shows the constant-voltage step at the 10 V level with high resolution.

for operation at 16 GHz generate voltages up to 17 V [63]. Another version for 70 GHz operation realized by Hassel *et al.* [79] is based on an improved design of 3315 externally shunted SIS junctions operated on the third-order constant-voltage step. Recently, 1 V SNIS arrays were developed by Lacquaniti *et al.* [80] using a slightly oxidized thick Al layer (up to 100 nm) as the barrier.

#### 7.1.4.1.3 Applications of Binary-Divided Arrays

Different applications of PJVSs in metrology have successfully been demonstrated. As these developments proceed very rapidly at present, only some basic ideas are briefly described. At first, PJVSs are also superior to conventional arrays for DC measurements, as they allow easier automation, faster polarity reversing, and thus lower uncertainties within a given measurement time [81–84].

PJVSs were originally intended for synthesizing AC voltages. However, first measurements soon revealed the difficulties in generating AC waveforms with low uncertainties as required for metrological purposes [85]. Major problems result from the transients between different constant-voltage steps. The voltage is not determined with sufficient accuracy during the switching between the steps (the voltage is not given by the Josephson equation here) [86]. Although improvements of the bias electronics significantly reduced the transients from about  $1 \mu\text{s}$  in 1997 [85] to below 100 ns in 2007 [87], measurements with thermal transfer standards demonstrated that metrological relevant uncertainties better than  $10^{-6}$  are possible only for frequencies below about 200 Hz. As the transients sensitively depend on many external data, further improvements will be very difficult as error analyses indicated [88, 89].

An idea for overcoming these limitations is the combination of PJVSs and sampling methods first introduced by Behr *et al.* in 2007 [90]. The combination of a PJVS and a sampling voltmeter results in an “AC quantum voltmeter” that enables the measurement of periodic waveforms up to audio frequencies. The sampling

voltmeter is used to measure the small difference between the AC signal and the reference voltage of the PJVS. Proper triggering is required to ensure sampling while the PJVS is on a constant-voltage step. Successful measurements have been demonstrated by several groups (cf. [91–95]) including the use of an automated 10 V AC quantum voltmeter in a calibration laboratory [96].

Further applications are impedance measurements by Josephson bridges [97], electrical power standards [84, 92, 98], and characterizations of A/D converters [99] among others. In addition, PJVSs have been successfully operated in cryocoolers (cf. [100, 101]).

#### 7.1.4.2 Pulse-Driven Arrays

The JVSs described so far are operated by sinusoidal microwaves. This works well, if the operating frequency is close to the characteristic frequency of the junctions (cf. Section 7.1.2.2; [4, 7, 15]). A modulation of the output voltage by changing the frequency of the irradiated microwaves over a wide frequency range is therefore not possible. Nevertheless, a direct time-dependent manipulation of the flux quanta transfer seems to be very promising for an AC JVS, in order to enable the synthesis of spectrally pure waveforms and to avoid those drawbacks related to the D/A converter operation of binary-divided arrays.

The limitations of sinusoidal operation do not appear, if the JJs are operated by a train of short current pulses as first shown by simulations [102, 103]. The width of the constant-voltage steps is nearly independent of the pulse repetition frequency between zero and the characteristic frequency, if rise and fall time of the pulses are short compared to the characteristic frequency (10 GHz corresponds to 100 ps). The train of pulses then determines the number of flux quanta transferred across the JJs at any time, that is, the waveform to be generated is encoded in the pulse train [43]. A high-pulse repetition rate generates high voltages; the voltage decreases with a decreasing pulse repetition rate. Arbitrary waveforms can be synthesized by modulating the pulse train using a pulse pattern generator; sometimes this version of pulse-driven Josephson arrays is therefore called *JAWS*.

The pulse train is typically created by the use of a first- or second-order sigma-delta modulation [104, 105]. This procedure shifts the quantization noise to high frequencies; noise contributions are then removed by appropriate filtering. The JJs act as a perfect quantizer due to the transfer of flux quanta. Spectrally pure waveforms with higher harmonics suppressed by more than 100 dB are synthesized that way (cf. [105, 106] achieving root mean square (rms) output voltages of 1 V recently [107, 108]).

##### 7.1.4.2.1 Design of Pulse-Driven Arrays

As the pulses consist of broadband frequency components ranging from DC to about 30 GHz, a complex microwave assembly is required in order to enable the transmission of these signals. Because of the difficulties to homogeneously propagate the pulse train, the circuits should be as small as possible. As a consequence, the size of the single junction lies in the range from 1 to 10  $\mu\text{m}^2$ , which is smaller

than that for conventional and PJVSs. The junctions often realized as double- or triple-stacked junctions are embedded into the middle of a CPW (cf. [105–108]).

#### 7.1.4.2.2 Realization of Pulse-Driven Arrays

Pulse-driven arrays were suggested and first demonstrated by Benz and Hamilton at NIST in 1996 [43]. An array of 512 SNS AuPd JJs operated by unipolar pulses with a repetition frequency up to 250 MHz generated constant-voltage steps up to 265  $\mu\text{V}$ . Continuous enhancements gradually improved the spectra of the synthesized signals and increased the output voltages. The first important steps of improvements were also suggested by Benz *et al.*: a code generator allowing a pulse repetition frequency of about 10 GHz in 1998 [104], the use of a bipolar drive signal in 1999 [109], and the AC coupling technique for operation of extended arrays in 2001 [110]. Further improvements resulted in rms voltages up to 275 mV generated by simultaneous operation of two arrays containing 6400  $\text{Nb}_x\text{Si}_{1-x}$  JJs each [106].

The overdamped JJs required for pulse-driven arrays are predominately realized by SNS junctions nowadays. Different materials have been used for the barrier such as PdAu [110], HfTi [111], or  $\text{Nb}_x\text{Si}_{1-x}$  [112, 113]. Besides, SINIS JJs have been investigated [114, 115]. While the superconductive layers of the JJs for pulse-driven arrays are typically made from Nb, JJs based on NbN/TiN have also been used [115].

The pulse train is typically provided by a commercial pulse pattern generator (bitstream generator). As bipolar signals are preferred for metrological applications, ways and means have been investigated to generate bipolar pulse trains even with unipolar pulse generators initially available. Benz *et al.* [109] suggested the appropriate superposition of a high-frequency sine wave and a two-level digital signal of a generator delivering unipolar pulses for this purpose in 1999. Improved and modified pulse-bias electronics based on this superposition are used at NIST to date [116]. Three-level code generators being commercially available today are alternatives (cf. [117]); they make the direct generation of bipolar pulses possible additionally resulting in less complex measurement setups. Improved pulse-bias techniques have also been suggested and investigated (cf. [116, 118]).

Because of the complex pulse operation, each single array presently requires the drive by one pulse source; a simple splitting of a large series array into several parallel microwave branches is not possible for pulse-driven arrays. As most commercial pulse pattern generators contain only two output channels, only two series arrays could be operated simultaneously, which limited for a long time the maximum output voltage to about 275 mV (rms) by operation of two arrays containing 6400  $\text{Nb}_x\text{Si}_{1-x}$  barrier junctions each [106]. A major breakthrough was the demonstration of 1 V waveforms by the groups at NIST and at PTB in 2014 [107, 108]. Novel pulse pattern generators with four or even eight output channels allowed the simultaneous operation of four or eight arrays containing a total of 51 200 or 63 000  $\text{Nb}_x\text{Si}_{1-x}$  barrier JJs, respectively. Figure 7.1.6 shows a synthesized sine wave with an rms output voltage of 1 V and the corresponding frequency spectrum.

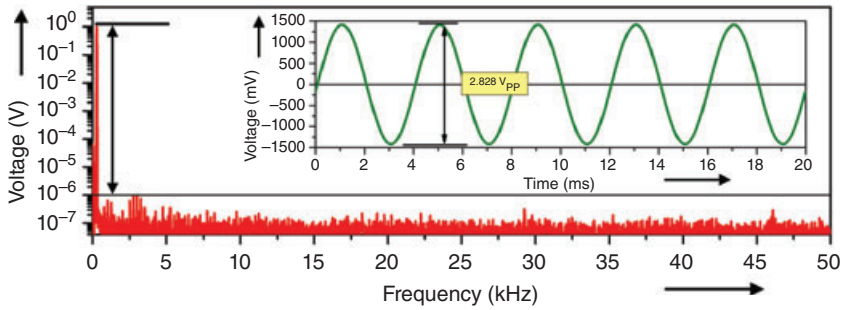


**Figure 7.1.6** Frequency spectrum of a synthesized sine wave (inset) with an rms output voltage of 1 V (peak-to-peak voltage of 2.828 V) at a frequency of 250 Hz. Higher harmonics are suppressed by more than 120 dB. Eight Josephson arrays containing a total of 63 000  $\text{Nb}_x\text{Si}_{1-x}$  barrier JJs were simultaneously operated at PTB (cf. [119]).

Using pulse-driven arrays, different waveforms have been synthesized over a wide frequency range from about 10 Hz to 1 MHz; higher harmonics are typically suppressed by more than 120 dBc (cf. [106, 107, 119–121]). The operation margins of the arrays have been significantly improved to more than 2 mA at 1 V (cf. [107]). The operation of pulse-driven Josephson arrays in a cryocooler (cf. [113, 122]) enables shorter wires for the output signals, which reduces the problems when synthesizing waveforms above about 100 kHz (cf. [123]).

Comparisons between the output voltages of a pulse-driven and a binary-divided JVS showed an excellent agreement of both systems; the relative uncertainties have been improved with increasing voltages of the comparisons from  $5 \times 10^{-7}$  at 8 mV [124] to  $2.6 \times 10^{-7}$  at 104 mV [125] and  $2.4 \times 10^{-8}$  at 1 V [119] ( $k=2$ ). In addition, Kieler *et al.* [113] performed a direct comparison of two sine waves synthesized by two pulse-driven arrays demonstrating an excellent agreement of both voltages of  $(1.6 \pm 5.8) \times 10^{-8}$  ( $k=2$ ).

#### 7.1.4.2.3 Applications of Pulse-Driven Arrays

The arbitrary perfect waveforms synthesized by pulse-driven arrays are very useful for different metrological applications, some of which are briefly described here. First of all, pulse-driven arrays were used as synthesizers for arbitrary waveforms up to 1 MHz with very pure frequency spectra and quantum-accurate voltages (cf. [105–108, 121]). Moreover, pulse-driven arrays were utilized for calibrations of thermal converters and transfer standards (cf. [106, 126]). Single- or multitone signals were also used for the characterization of electronic components such as filters or A/D converters (cf. [127]). To reach higher voltages at least for low frequencies, PTB suggested and realized the use of pulse-driven arrays in combination with a binary-divided array [128, 129]; the spectrum of the pulse-driven array is adjusted to suppress the higher harmonics in the spectrum of the 1 or 10 V signal generated by the binary-divided array [129]. The use of the pulse-driven 1 V system is at the beginning [107, 108]; several applications are expected here. In addition, pulse-driven arrays provide the opportunity for synthesizing a

calculable pseudonoise waveform consisting of a comb of random-phase harmonics, each having identical voltage amplitude. A low-voltage version of this noise source is used for high-precision measurements of the Boltzmann constant with a quantum-based Johnson noise thermometry system measuring the voltage noise of the resistor and thus its temperature [130, 131].

Most of these very encouraging results have been achieved using pulse pattern generators, which are based on semiconductor electronics and are mostly commercially available. The high-frequency pulses are transmitted by semirigid coax cables to the JJs at 4.2 K. Operation of JJs by optical pulses has been also investigated; transmission of the pulses through optical fibers might simplify the operation of multiple Josephson arrays. The approach of Kohlmann *et al.* [114] is based on balanced photodiodes arranged at each array and operated by short optical pulses [132]. The operation of Josephson arrays by optical pulses has also been investigated by Urano *et al.* [115, 133].

### 7.1.5

#### Conclusions

About 50 years after the discovery of the Josephson effects, JVSs are nowadays well established as famous application of superconductive electronics in electrical metrology. This long time of developments was needed to progress from single junctions delivering a few millivolts at most to highly integrated series arrays containing thousands of JJs that generate voltages of more than 10 V. Advanced fabrication technologies are an essential precondition for these remarkable developments. In 1990, JVSs were adopted for the representation of the unit of voltage, the volt.

Conventional 10 V JVSs are well established for DC measurements and are commercially available. PJVSs opened up the world of AC applications and have, hence, been the next step in the exciting story of the applications of the Josephson effect in metrology. 10 V arrays containing tens or even hundreds of thousands of JJs are meanwhile fabricated routinely. In future, conventional JVSs will be replaced more and more by PJVSs, as they are easier to operate and provide additional exciting possibilities and applications. Pulse-driven arrays enable the synthesis of real quantum-based AC voltages. While their output voltages were limited to 275 mV for several years, a major breakthrough was achieved in 2014 by synthesizing waveforms with rms output voltages of 1 V. Initial applications have impressively demonstrated the potential of binary-divided and pulse-driven JVSs. Further developments will establish these JVSs as a quantum basis for AC metrology.

#### Acknowledgments

The exciting story of JVSs have been written by many researchers. I would like to thank Jürgen Niemeyer, Ralf Behr, and the whole JVS team at PTB, as well as



national and international colleagues in this field for many discussions, comments, and support. The work has been also supported in part within national and international research projects.

## References

- Josephson, B.D. (1962) Possible new effects in superconductive tunnelling. *Phys. Lett.*, **1** (7), 251–253.
- Anders, S., Blamire, M.G., Buchholz, F.-I. *et al* (2010) European roadmap on superconductive electronics – status and perspectives. *Physica C*, **470** (23–24), 2079–2126.
- Niemeyer, J. (1989) in *Superconducting Quantum Electronics* (ed. V. Kose), Springer, Berlin, pp. 228–254.
- Kautz, R.L. (1992) in *Metrology at the Frontiers of Physics and Technology* (eds L. Crovini and T.J. Quinn), North-Holland, Amsterdam, pp. 259–296.
- Niemeyer, J. (1998) in *Handbook of Applied Superconductivity* (ed. B. Seeber), Institute of Physics Publishing, Bristol, pp. 1813–1834.
- Yoshida, H. (2000) Application of the ac Josephson effect for precise measurements. *IEICE Trans. Electron.*, **E83-C** (1), 20–26.
- Kautz, R.L. (1996) Noise, chaos, and the Josephson voltage standard. *Rep. Prog. Phys.*, **59** (8), 935–992.
- Hamilton, C.A. (2000) Josephson voltage standards. *Rev. Sci. Instrum.*, **71** (10), 3611–3623.
- Behr, R., Müller, F., and Kohlmann, J. (2002) in *Studies of Josephson Junction Arrays II: Studies of High Temperature Superconductors*, vol. **40** (ed. A.V. Narlikar), Nova Science Publishers, Hauppauge, NY, pp. 155–184.
- Kohlmann, J., Behr, R., and Funck, T. (2003) Josephson voltage standards. *Meas. Sci. Technol.*, **14** (8), 1216–1228.
- Benz, S.P. and Hamilton, C.A. (2004) Application of the Josephson effect to voltage metrology. *Proc. IEEE*, **92** (10), 1617–1629.
- Jeanneret, B. and Benz, S.P. (2009) Applications of the Josephson effect in electrical metrology. *Eur. Phys. J. Spec. Top.*, **172**, 181–206.
- Kohlmann, J. and Behr, R. (2011) in *Superconductivity – Theory and Applications* (ed. A. Moysés Luiz), InTech, Rijeka, pp. 239–260, dx.doi.org/10.5772/17031 (accessed 21 June).
- Behr, R., Kieler, O., Kohlmann, J., Müller, F., and Palafox, L. (2012) Development and metrological applications of Josephson arrays at PTB. *Meas. Sci. Technol.*, **23** (12), 124002 (19 pp).
- Kautz, R.L. (1995) Shapiro steps in large-area metallic-barrier Josephson junctions. *J. Appl. Phys.*, **78** (9), 5811–5819.
- Harris, R.E. and Niemeyer, J. (2011) in *100 Years of Superconductivity* (eds H. Rogalla and P. Kes), Taylor & Francis, Boca Raton, FL, pp. 515–557.
- Josephson, B.D. (1965) Supercurrents through barriers. *Adv. Phys.*, **14** (56), 419–451.
- Rogalla, H. (1998) in *Handbook of Applied Superconductivity* (ed. B. Seeber), Institute of Physics Publishing, Bristol, pp. 1759–1775.
- Barone, A. and Paternò, G. (1982) *Physics and Applications of the Josephson Effect*, John Wiley & Sons, Inc., New York.
- Likharev, K.K. (1984) *Dynamics of Josephson Junctions and Circuits*, Gordon and Breach Science Publishers, New York.
- Kadin, A.M. (1999) *Introduction to Superconducting Circuits*, John Wiley & Sons, Inc., New York.
- Bureau International des Poids et Mesures (2006) *The International System of Units (SI)*, 8th edn, BIPM, www.bipm.org/en/si/si\_brochure/ (accessed 15 May 2014).
- Funck, T. and Sienknecht, V. (1991) Determination of the volt with the improved PTB voltage balance. *IEEE Trans. Instrum. Meas.*, **40** (2), 158–161.

24. Mills, I.M., Mohr, P.J., Quinn, T.J., Taylor, B.N., and Williams, E.R. (2006) Redefinition of the kilogram, ampere, kelvin and mole: a proposed approach to implementing CIPM recommendation 1 (CI-2005). *Metrologia*, **43** (3), 227–246.
25. Froehlich, M. (1978) *Das Normalelement*, Akademische Verlagsgesellschaft, Wiesbaden.
26. Terrien, J. (1973) News from the Bureau International des Poids et Mesures. *Metrologia*, **9** (1), 40–43.
27. Taylor, B.N. and Witt, T.J. (1989) New international electrical reference standards based on the Josephson and quantum Hall effects. *Metrologia*, **26** (1), 47–62.
28. Quinn, T.J. (1989) News from the BIPM. *Metrologia*, **26** (1), 69–74.
29. Bardeen, J., Cooper, L.N., and Schrieffer, J.R. (1957) Theory of superconductivity. *Phys. Rev.*, **108** (5), 1175–1204.
30. Shapiro, S. (1963) Josephson currents in superconducting tunneling: the effect of microwaves and other observations. *Phys. Rev. Lett.*, **11** (2), 80–82.
31. Stewart, W.C. (1968) Current-voltage characteristics of Josephson junctions. *Appl. Phys. Lett.*, **12** (8), 277–280.
32. McCumber, D.E. (1968) Effect of ac impedance on dc voltage-current characteristics of superconductor weak-link junctions. *J. Appl. Phys.*, **39** (7), 3113–3118.
33. Taylor, B.N., Parker, W.H., Langenberg, D.N., and Denenstein, A. (1967) On the use of the ac Josephson effect to maintain standards of electromotive force. *Metrologia*, **3** (4), 89–98.
34. Clarke, J. (1968) Experimental comparison of the Josephson voltage-frequency relation in different superconductors. *Phys. Rev. Lett.*, **21** (23), 1566–1569.
35. Jain, A.K., Lukens, J.E., and Tsai, J.S. (1987) Test for relativistic gravitational effects on charged particles. *Phys. Rev. Lett.*, **58** (12), 1165–1168.
36. Endo, T., Koyanagi, M., and Nakamura, A. (1983) High-accuracy Josephson potentiometer. *IEEE Trans. Instrum. Meas.*, **32** (1), 267–271.
37. Pöpel, R. (1992) The Josephson effect and voltage standards. *Metrologia*, **29** (2), 153–174.
38. Levinsen, M.T., Chiao, R.Y., Feldman, M.J., and Tucker, B.A. (1977) An inverse ac Josephson effect voltage standard. *Appl. Phys. Lett.*, **31** (11), 776–778.
39. Niemeyer, J., Hinken, J.H., and Kautz, R.L. (1984) Microwave-induced constant-voltage steps at one volt from a series array of Josephson junctions. *Appl. Phys. Lett.*, **45** (4), 478–480.
40. Lloyd, F., Hamilton, C.A., Beall, J., Go, D., Ono, R.H., and Harris, R.E. (1987) A Josephson array voltage standard at 10 V. *IEEE Electron Device Lett.*, **8** (10), 449–450.
41. Pöpel, R., Niemeyer, J., Fromknecht, R., Meier, W., and Grimm, L. (1990) 1- and 10-V series array Josephson voltage standards in Nb/Al<sub>2</sub>O<sub>3</sub>/Nb technology. *J. Appl. Phys.*, **68** (8), 4294–4303.
42. Hamilton, C.A., Burroughs, C.J., and Kautz, R.L. (1995) Josephson D/A converter with fundamental accuracy. *IEEE Trans. Instrum. Meas.*, **44** (2), 223–225.
43. Benz, S.P. and Hamilton, C.A. (1996) A pulse-driven programmable Josephson voltage standard. *Appl. Phys. Lett.*, **68** (22), 3171–3173.
44. Müller, F., Pöpel, R., Kohlmann, J., Niemeyer, J., Meier, W., Weimann, T., Grimm, L., Dünschede, F.-W., and Gutmann, P. (1997) Optimized 1 V and 10 V Josephson series arrays. *IEEE Trans. Instrum. Meas.*, **46** (2), 229–232.
45. Hamilton, C.A. and Burroughs, C.J. (1995) Performance and reliability of NIST 10-V Josephson arrays. *IEEE Trans. Instrum. Meas.*, **44** (2), 238–240.
46. Endo, T., Sakamoto, Y., Murayama, Y., Iwasa, A., and Yoshida, H. (1995) 1-V Josephson-junction-array voltage standard and development of 10-V Josephson junction array at ETL. *IEICE Trans. Electron.*, **E78-A** (5), 503–510.
47. Radparvar, M. (1995) Superconducting niobium and niobium nitride processes for medium-scale integration applications. *Cryogenics*, **35** (8), 535–540.
48. Meyer, H.-G., Wende, G., Fritzsche, L., Thrum, F., Schubert, M., Müller, F., Behr, R., and Niemeyer, J. (1999) Improved primary Josephson voltage

- standard with a new microwave driving source. *IEEE Trans. Appl. Supercond.*, **9** (2), 4150–4153.
49. Schubert, M., May, T., Wende, G., Fritzsche, L., and Meyer, H.-G. (2001) Coplanar strips for Josephson voltage standard circuits. *Appl. Phys. Lett.*, **79** (7), 1009–1011.
  50. Gurvitch, M., Washington, W.A., and Huggins, H.A. (1983) High quality refractory Josephson tunnel junctions utilizing thin aluminium layers. *Appl. Phys. Lett.*, **42** (5), 472–474.
  51. Niemeyer, J., Sakamoto, Y., Vollmer, E., Hinken, J.H., Shoji, A., Nakagawa, H., Takada, S., and Kosaka, S. (1986) Nb/Al-oxide/Nb and NbN/MgO/NbN tunnel junctions in large series arrays for voltage standards. *Jpn. J. Appl. Phys.*, **25** (5), L343–L345.
  52. Wood, B. and Solve, S. (2009) A review of Josephson comparison results. *Metrologia*, **46** (6), R13–R20.
  53. Giem, J.I. (1991) Sub-ppm linearity testing of a DMM using a Josephson junction array. *IEEE Trans. Instrum. Meas.*, **40** (2), 329–332.
  54. BIPM BIPM Database, <http://kcdb.bipm.org/> (accessed 15 June 2014).
  55. Semenov, V.K. and Polyakov, Y.A. (2001) Circuit improvements for a voltage multiplier. *IEEE Trans. Appl. Supercond.*, **11** (1), 550–553.
  56. Benz, S.P. (1995) Superconductor-normal-superconductor junctions for programmable voltage standards. *Appl. Phys. Lett.*, **67** (18), 2714–2716.
  57. Benz, S.P., Hamilton, C.A., Burroughs, C.J., Harvey, T.E., and Christian, L.A. (1997) Stable 1-volt programmable voltage standard. *Appl. Phys. Lett.*, **71** (13), 1866–1868.
  58. Dresselhaus, P.D., Elsbury, M.M., and Benz, S.P. (2009) Tapered transmission lines with dissipative junctions. *IEEE Trans. Appl. Supercond.*, **19** (3), 993–998.
  59. Schulze, H., Müller, F., Behr, R., Kohlmann, J., Niemeyer, J., and Balashov, D. (1999) SINIS Josephson junctions for programmable Josephson voltage standard circuits. *IEEE Trans. Appl. Supercond.*, **9** (2), 4241–4244.
  60. Burroughs, C.J., Rüfenacht, A., Dresselhaus, P.D., Benz, S.P., and Elsbury, M.M. (2009) A 10 volt “turnkey” programmable Josephson voltage standard for DC and stepwise-approximated waveforms. *NCSLI Meas.*, **4** (3), 70–75.
  61. Schubert, M., Fritzsche, L., Wende, G., and Meyer, H.-G. (2001) SNS junction on Nb-Ti base for microwave circuits. *IEEE Trans. Appl. Supercond.*, **11** (1), 1066–1069.
  62. Chong, Y., Burroughs, C.J., Dresselhaus, P.D., Hadacek, N., Yamamori, H., and Benz, S.P. (2005) Practical high-resolution programmable Josephson voltage standards using double- and triple-stacked MoSi<sub>2</sub>-barrier junctions. *IEEE Trans. Appl. Supercond.*, **15** (2), 461–464.
  63. Yamamori, H., Yamada, T., Sasaki, H., and Shoji, A. (2008) 10 V programmable Josephson voltage standard circuit with a maximum output voltage of 20 V. *Supercond. Sci. Technol.*, **21** (10), 105007 (6 pp).
  64. Baek, B., Dresselhaus, P.D., and Benz, S.P. (2006) Co-Sputtered amorphous Nb<sub>x</sub>Si<sub>1-x</sub> barriers for Josephson-junction circuits. *IEEE Trans. Appl. Supercond.*, **16** (4), 1966–1970.
  65. Hertel, G., Bishop, D.J., Spencer, E.G., Rowell, J.M., and Dynes, R.C. (1983) Tunneling and transport measurements at the metal–insulator transition of amorphous Nb:Si. *Phys. Rev. Lett.*, **50** (10), 743–746.
  66. Burroughs, C.J., Dresselhaus, P.D., Rüfenacht, A., Olaya, D., Elsbury, M.M., Tang, Y.-H., and Benz, S.P. (2011) NIST 10 V programmable Josephson voltage standard system. *IEEE Trans. Instrum. Meas.*, **60** (7), 2482–2488.
  67. Elsbury, M.M., Dresselhaus, P.D., Bergren, N.F., Burroughs, C.J., Benz, S.P., and Popovic, Z. (2009) Broadband lumped-element integrated-way power dividers for voltage standards. *IEEE Trans. Microwave Theory Tech.*, **57** (8), 2055–2063.
  68. Dresselhaus, P.D., Elsbury, M.M., Olaya, D., Burroughs, C.J., and Benz, S.P. (2011) 10 V programmable Josephson

- voltage standard circuits using NbSi-barrier junctions. *IEEE Trans. Appl. Supercond.*, **21** (3), 693–696.
69. Fox, A.E., Dresselhaus, P.D., Rüfenacht, A., Sanders, A., and Benz, S.P. (2015) Junction yield analysis for 10 V programmable Josephson voltage standard devices. *IEEE Trans. Appl. Supercond.*, **25** (3), 1101505 (5 pp).
  70. Maezawa, M. and Shoji, A. (1997) Overdamped Josephson junctions with Nb/AIO<sub>x</sub>/Al/AIO<sub>x</sub>/Nb structure for integrated circuit application. *Appl. Phys. Lett.*, **70** (26), 3603–3605.
  71. Sugiyama, H., Yanada, A., Ota, M., Fujimaki, A., and Hayakawa, H. (1997) Characteristics of Nb/AIO<sub>x</sub>/Al/AIO<sub>x</sub>/Nb junctions based on the proximity effect. *Jpn. J. Appl. Phys.*, **36** (9A/B), L1157–L1160.
  72. Schulze, H., Behr, R., Müller, F., and Niemeyer, J. (1998) Nb/Al/AIO<sub>x</sub>/Al/AIO<sub>x</sub>/Al/Nb Josephson junctions for programmable voltage standards. *Appl. Phys. Lett.*, **73** (7), 996–998.
  73. Behr, R., Schulze, H., Müller, F., Kohlmann, J., and Niemeyer, J. (1999) Josephson arrays at 70 GHz for conventional and programmable voltage standards. *IEEE Trans. Instrum. Meas.*, **48** (2), 270–273.
  74. Schulze, H., Behr, R., Kohlmann, J., Müller, F., and Niemeyer, J. (2000) Design and fabrication of 10 V SINIS Josephson arrays for programmable voltage standards. *Supercond. Sci. Technol.*, **13** (9), 1293–1295.
  75. Müller, F., Behr, R., Palafox, L., Kohlmann, J., Wendisch, R., and Krasnopolin, I. (2007) Improved 10 V SINIS series arrays for applications in AC voltage metrology. *IEEE Trans. Appl. Supercond.*, **17** (2), 649–652.
  76. Mueller, F., Behr, R., Weimann, T., Palafox, L., Olaya, D., Dresselhaus, P.D., and Benz, S.P. (2009) 1 V and 10 V SNS programmable voltage standards for 70 GHz. *IEEE Trans. Appl. Supercond.*, **19** (3), 981–986.
  77. Müller, F., Scheller, T., Wendisch, R., Behr, R., Kieler, O., Palafox, L., and Kohlmann, J. (2013) NbSi barrier junctions tuned for metrological applications up to 70 GHz: 20 V arrays for programmable Josephson voltage standards. *IEEE Trans. Appl. Supercond.*, **23** (3), 1101005 (5 pp).
  78. Yamamori, H., Ishizaki, M., Shoji, A., Dresselhaus, P.D., and Benz, S.P. (2006) 10 V programmable Josephson voltage standard circuits using NbN/TiN<sub>x</sub>/NbN/TiN<sub>x</sub>/NbN double-junction stacks. *Appl. Phys. Lett.*, **88** (4), 042503 (3 pp).
  79. Hassel, J., Helistö, P., Grönberg, L., Seppä, H., Nissilä, J., and Kemppinen, A. (2005) Stimulated power generation in ES-SIS junction arrays. *IEEE Trans. Instrum. Meas.*, **54** (2), 632–635.
  80. Lacquaniti, V., de Leo, N., Fretto, M., Sosso, A., Müller, F., and Kohlmann, J. (2011) 1 V programmable voltage standards based on SNIS Josephson junction series arrays. *Supercond. Sci. Technol.*, **24** (4), 045004 (4 pp).
  81. Burroughs, C.J., Benz, S.P., Hamilton, C.A., Harvey, T.E., Kinard, J.R., Lipe, T.E., and Sasaki, H. (1999) Thermoelectric transfer difference of thermal converters measured with a Josephson source. *IEEE Trans. Instrum. Meas.*, **48** (2), 282–284.
  82. Behr, R., Grimm, L., Funck, T., Kohlmann, J., Schulze, H., Müller, F., Schumacher, B., Warnecke, P., and Niemeyer, J. (2001) Application of Josephson series arrays for a dc quantum voltmeter. *IEEE Trans. Instrum. Meas.*, **50** (2), 185–187.
  83. Behr, R., Funck, T., Schumacher, B., and Warnecke, P. (2003) Measuring resistance standards in terms of the quantized Hall resistance with a dual Josephson voltage standard using SINIS Josephson arrays. *IEEE Trans. Instrum. Meas.*, **52** (2), 521–523.
  84. Palafox, L., Behr, R., Ihlenfeld, W.G.K., Müller, F., Mohns, E., Seckelmann, M., and Ahlers, F. (2009) The Josephson-effect-based primary AC power standard at the PTB: a progress report. *IEEE Trans. Instrum. Meas.*, **58** (4), 1049–1053.
  85. Hamilton, C.A., Burroughs, C.J., Benz, S.P., and Kinard, J.R. (1997) AC Josephson voltage standard: progress report.

- IEEE Trans. Instrum. Meas.*, **46** (2), 224–228.
86. Hamilton, C.A., Burroughs, C.J., and Benz, S.P. (1997) Josephson voltage standard – a review. *IEEE Trans. Appl. Supercond.*, **7** (2), 3756–3761.
  87. Williams, J.M., Henderson, D., Patel, P., Behr, R., and Palafox, L. (2007) Achieving sub-100-ns switching of programmable Josephson arrays. *IEEE Trans. Instrum. Meas.*, **56** (2), 651–654.
  88. Burroughs, C.J., Rüfenacht, A., Benz, S.P., and Dresselhaus, P.D. (2009) Systematic error analysis of stepwise-approximated ac waveforms generated by programmable Josephson voltage standards. *IEEE Trans. Instrum. Meas.*, **58** (4), 761–767.
  89. Lee, J., Behr, R., Katkov, A.S., and Palafox, L. (2009) Modeling and measuring error contributions in stepwise synthesized sine waves. *IEEE Trans. Instrum. Meas.*, **58** (4), 803–808.
  90. Behr, R., Palafox, L., Ramm, G., Moser, H., and Melcher, J. (2007) Direct comparison of Josephson waveforms using an AC quantum voltmeter. *IEEE Trans. Instrum. Meas.*, **56** (2), 235–238.
  91. Lee, J., Behr, R., Palafox, L., Katkov, A., Schubert, M., Starkloff, M., and Böck, A.C. (2013) An ac quantum voltmeter based on 10 V programmable Josephson array. *Metrologia*, **50** (6), 612–622.
  92. Rüfenacht, A., Burroughs, C.J., Dresselhaus, P.D., and Benz, S.P. (2013) Differential sampling measurement of a 7 V rms sine wave with a programmable Josephson voltage standard. *IEEE Trans. Instrum. Meas.*, **62** (6), 1587–1593.
  93. Kim, M.-S., Kim, K.-T., Kim, W.-S., Chong, Y., and Kwon, S.-W. (2010) Analog-to-digital conversion for low-frequency waveforms based on the Josephson voltage standard. *Meas. Sci. Technol.*, **21** (11), 115102 (6 pp).
  94. Williams, J.M., Henderson, D., Pickering, J., Behr, R., Müller, F., and Scheibenreiter, P. (2011) Quantum-referenced voltage waveform synthesizer. *IET Sci. Meas. Technol.*, **5** (5), 167–174.
  95. Rüfenacht, A., Overney, F., Mortara, A., and Jeanneret, B. (2011) Thermal-transfer standard validation of the Josephson-voltage-standard-locked sine-wave synthesizer. *IEEE Trans. Instrum. Meas.*, **60** (7), 2372–2377.
  96. Schubert, M., Starkloff, M., Lee, J., Behr, R., Palafox, L., Wintermeier, A., Böck, A.C., Fleischmann, P.M., and May, T. (2015) An AC Josephson voltage standard up to the kilohertz range tested in a calibration laboratory. *IEEE Trans. Instrum. Meas.*, **64** (6), 1620–1626.
  97. Lee, J., Schurr, J., Nissilä, J., Palafox, L., Behr, R., and Kibble, B.P. (2011) Programmable Josephson arrays for impedance measurements. *IEEE Trans. Instrum. Meas.*, **60** (7), 2596–2601.
  98. Palafox, L., Ramm, G., Behr, R., Ihlenfeld, W.G.K., Müller, F., and Moser, H. (2007) Primary AC power standard based on programmable Josephson junction arrays. *IEEE Trans. Instrum. Meas.*, **56** (2), 534–537.
  99. Ihlenfeld, W.G.K., Mohns, E., Behr, R., Williams, J., Patel, P., Ramm, G., and Bachmair, H. (2005) Characterization of a high resolution analog-to-digital converter with a Josephson AC voltage source. *IEEE Trans. Instrum. Meas.*, **54** (2), 649–652.
  100. Rüfenacht, A., Howe, L.A., Fox, A.E., Schwall, R.E., Dresselhaus, P.D., Burroughs, C.J., and Benz, S.P. (2015) Cryocooled 10 V programmable Josephson voltage standard. *IEEE Trans. Instrum. Meas.*, **64** (6), 1477–1482.
  101. Maruyama, M., Iwasa, A., Yamamori, H., Chen, S.-F., Urano, C., and Kaneko, N. (2015) Calibration system for Zener voltage standards using 10 V programmable Josephson voltage standard at NMIJ. *IEEE Trans. Instrum. Meas.*, **64** (6), 1606–1612.
  102. Monaco, R. (1990) Enhanced ac Josephson effect. *J. Appl. Phys.*, **68** (2), 679–687.
  103. Maggi, S. (1995) RF-induced steps in a pulse driven Josephson junction. *Inst. Phys. Conf. Ser.*, **148**, 1243–1246.
  104. Benz, S.P., Hamilton, C.A., Burroughs, C.J., Harvey, T.E., Christian, L.A., and Przybysz, J.X. (1998) Pulse-driven Josephson digital/analog converter. *IEEE Trans. Appl. Supercond.*, **8** (2), 42–47.
  105. Kieler, O.F., Iuzzolino, R., and Kohlmann, J. (2009) Sub- $\mu\text{m}$  SNS

- Josephson junction arrays for the Josephson arbitrary waveform synthesizer. *IEEE Trans. Appl. Supercond.*, **19** (3), 230–233.
106. Benz, S.P., Dresselhaus, P.D., Rüfenacht, A., Bergren, N.F., Kinard, J.R., and Landim, R.P. (2009) Progress toward a 1 V pulse-driven AC Josephson voltage standard. *IEEE Trans. Instrum. Meas.*, **58** (4), 838–843.
  107. Benz, S.P., Waltman, S.B., Fox, A.E., Dresselhaus, P.D., Rüfenacht, A., Howe, L., Schwall, R.E., and Flowers-Jacobs, N.E. (2015) Performance improvements for the NIST 1 V Josephson arbitrary waveform synthesizer. *IEEE Trans. Appl. Supercond.*, **25** (3), 1400105 (5 pp).
  108. Kieler, O.F., Behr, R., Wendisch, R., Bauer, S., Palafox, L., and Kohlmann, J. (2015) Towards a 1 V Josephson arbitrary waveform synthesizer. *IEEE Trans. Appl. Supercond.*, **25** (3), 1400305 (5 pp).
  109. Benz, S.P., Hamilton, C.A., Burroughs, C.J., and Harvey, T.E. (1999) AC and DC bipolar voltage source using quantized pulses. *IEEE Trans. Instrum. Meas.*, **48** (2), 266–269.
  110. Benz, S.P., Burroughs, C.J., and Dresselhaus, P.D. (2001) AC coupling technique for Josephson waveform synthesis. *IEEE Trans. Appl. Supercond.*, **11** (1), 612–616.
  111. Hagedorn, D., Kieler, O., Dolata, R., Behr, R., Müller, E., Kohlmann, J., and Niemeyer, J. (2006) Modified fabrication of planar sub- $\mu\text{m}$  superconductor-normal metal-superconductor Josephson junctions for use in a Josephson arbitrary waveform synthesizer. *Supercond. Sci. Technol.*, **19** (4), 294–298.
  112. Benz, S.P., Dresselhaus, P.D., Burroughs, C.J., and Bergren, N.F. (2007) Precision measurements using a 300 mV Josephson arbitrary waveform synthesizer. *IEEE Trans. Appl. Supercond.*, **17** (2), 864–869.
  113. Kieler, O.F., Behr, R., Schlessner, D., Palafox, L., and Kohlmann, J. (2013) Precision comparison of sine waveforms with pulse-driven Josephson arrays. *IEEE Trans. Appl. Supercond.*, **23** (3), 1301404 (4 pp).
  114. Kohlmann, J., Müller, F., Behr, R., Hagedorn, D., Kieler, O., Palafox, L., and Niemeyer, J. (2006) Development of Josephson junction series arrays for synthesis of AC voltages and arbitrary waveforms. *J. Phys. Conf. Ser.*, **43** (1), 1385–1388.
  115. Urano, C., Maruyama, M., Kaneko, N., Yamamori, H., Shoji, A., Maezawa, M., Hashimoto, Y., Suzuki, H., Nagasawa, S., Satoh, T., Hidaka, M., and Kiryu, S. (2009) Operation of a Josephson arbitrary waveform synthesizer with optical data input. *Supercond. Sci. Technol.*, **22** (11), 114012 (4 pp).
  116. Benz, S.P. and Waltman, S.B. (2014) Pulse-bias electronics and techniques for a Josephson arbitrary waveform synthesizer. *IEEE Trans. Appl. Supercond.*, **24** (6), 1400107 (7 pp).
  117. van den Brom, H.E., Houtzager, E., Brinkmeier, B.E.R., and Chevtchenko, O.A. (2008) Bipolar pulse-drive electronics for a Josephson arbitrary waveform synthesizer. *IEEE Trans. Instrum. Meas.*, **57** (2), 428–431.
  118. Zhou, K., Qu, J.F., and Benz, S.P. (2015) Zero-compensation method and reduced inductive voltage error for the AC Josephson voltage standard. *IEEE Trans. Appl. Supercond.*, **25** (5), 1400806 (6 pp).
  119. Behr, R., Kieler, O., Lee, J., Bauer, S., Palafox, L., and Kohlmann, J. (2015) Direct comparison of a 1 V Josephson arbitrary waveform synthesizer and an ac quantum voltmeter. *Metrologia*, **52** (4), 528–537.
  120. Kieler, O., Schlessner, D., Kohlmann, J., and Behr, R. (2010) Josephson arbitrary waveform synthesizer for analysis of AC components. 2010 Conference on Digest Precision Electromagnetic Measurements (CPEM) Digest, pp. 157–158.
  121. Houtzager, E., Benz, S.P., and van den Brom, H.E. (2009) Operating margins for a pulse-driven Josephson arbitrary waveform synthesizer using a ternary bit-stream generator. *IEEE Trans. Instrum. Meas.*, **58** (4), 775–780.
  122. Kieler, O.F.O., Scheller, T., and Kohlmann, J. (2013) Cryocooler operation of a pulse-driven AC Josephson

- voltage standard at PTB. *World J. Condens. Matter Phys.*, **3** (4), 189–193.
123. Filipinski, P.S., Boecker, M., Benz, S.P., and Burroughs, C.J. (2011) Experimental determination of the voltage lead error in an AC Josephson voltage standard. *IEEE Trans. Instrum. Meas.*, **60** (7), 2387–2392.
  124. Kohlmann, J., Kieler, O.F., Iuzzolino, R., Lee, J., Behr, R., Egeling, B., and Müller, F. (2009) Development and investigation of SNS Josephson arrays for the Josephson arbitrary waveform synthesizer. *IEEE Trans. Instrum. Meas.*, **58** (4), 797–802.
  125. Jeanneret, B., Rüfenacht, A., Overney, F., van den Brom, H., and Houtzager, E. (2011) High precision comparison between a programmable and a pulse-driven Josephson voltage standard. *Metrologia*, **48** (5), 311–316.
  126. Lipe, T.E., Kinard, J.R., Tang, Y.-H., Benz, S.P., Burroughs, C.J., and Dresselhaus, P.D. (2008) Thermal voltage converter calibrations using a quantum ac standard. *Metrologia*, **45** (3), 275–280.
  127. Toonen, R.C. and Benz, S.P. (2009) Nonlinear behavior of electronic components characterized with precision multitones from a Josephson arbitrary waveform synthesizer. *IEEE Trans. Appl. Supercond.*, **19** (3), 715–718.
  128. Kohlmann, J., Müller, F., Kieler, O., Behr, R., Palafox, L., Kahmann, M., and Niemeyer, J. (2007) Josephson series arrays for programmable 10-V SINIS Josephson voltage standards and for Josephson arbitrary waveform synthesizers based on SNS junctions. *IEEE Trans. Instrum. Meas.*, **56** (2), 472–475.
  129. Behr, R., Kieler, O.F.O., Schleußner, D., Palafox, L., and Ahlers, F.-J. (2013) Combining Josephson systems for spectrally pure AC waveforms with large amplitudes. *IEEE Trans. Instrum. Meas.*, **62** (6), 1634–1639.
  130. Benz, S.P., Qu, J., Rogalla, H., White, D.R., Dresselhaus, P.D., Tew, W.L., and Nam, S.W. (2009) Improvements in the NIST Johnson noise thermometry system. *IEEE Trans. Instrum. Meas.*, **58** (4), 884–890.
  131. Qu, J.F., Benz, S.P., Pollarolo, A., Rogalla, H., Tew, W.L., White, R., and Zhou, K.L. (2015) Improved electronic measurement of the Boltzmann constant by Johnson noise thermometry. *Metrologia*, **52** (5), S242–S256.
  132. Williams, J.M., Janssen, T.J.B.M., Palafox, L., Humphreys, D.A., Behr, R., Kohlmann, J., and Müller, F. (2004) The simulation and measurement of the response of Josephson junctions to optoelectronically generated short pulses. *Supercond. Sci. Technol.*, **17** (6), 815–818.
  133. Urano, C., Maruyama, M., Kaneko, N., Yamamori, H., Shoji, A., Maezawa, M., Hashimoto, Y., Suzuki, H., Nagasawa, S., Satoh, T., Hidaka, M., and Kiryu, S. (2010) A new coding technique in serial data transmission and demodulation with Josephson junctions array. *J. Phys. Conf. Ser.*, **234** (4), 042037 (5 pp).